Towards an All-digital Time Scale

Stefania Römisch, Steven R. Jefferts, Thomas E. Parker

Time and Frequency Division
NIST
Boulder, CO USA
romisch@boulder.nist.gov

Abstract **— The implementation of an all-digital time scale is under way at NIST, by use of a novel 8-channel, all-digital phase measurement system based on subsampling techniques. The phase measurement system is used to compare output signals from several commercial atomic frequency standards; the phase differences between these signals, at different measurement times, will then be input to the algorithm used to generate the digital time scale. The subsampling technique allows the elimination of analog mixers in the system's front end, with their noise contributions, and yields performance that is comparable to or better than the present state of the art. Long-term (up to 80 days) comparisons of both common-clock performance and fractional frequency measurements between the latest generation of the digital measurement system and the commercially available system used in the implementation of UTC(NIST) are presented.**

I. Introduction

The implementation of a time scale requires the ability to compare the time evolution of several clock signals. The instantaneous absolute phase of each clock is expressed in seconds to account for the accumulation of more than one cycle (2π radians) of phase difference between two signals. The quantity used in the computation of time scales is still commonly called *phase* but is in fact indicated with *x* and defined according to (1) below:

$$x(t) = \frac{\varphi(t)}{2\pi\nu_0},\qquad(1)$$

where $\varphi(t)$ is the instantaneous phase of the signal in radians and ν_0 is the nominal frequency of the same signal.

The differences between the instantaneous phase of *n* different clocks with respect to a clock *r*, elected to be the reference for the time scale, are indicated as $x_i(t)-x_r(t)$ and are then used by a weighting algorithm that computes the instantaneous phase of a virtual clock, the *ensemble clock*.

The ensemble clock, calculated by use of the algorithm *at1e* at NIST, is the representation of a local time scale, *TA(t)*. At NIST there are two real-time time scales, called AT1 and TSC, computed separately (but using the same algorithm) from distinct measurements of the same set of commercial atomic standards comprising both hydrogen masers and cesium thermal-beam clocks.

A third time scale, called DIG, will be computed, using the same algorithm, from the phase measurements on the same set of commercial atomic standards as executed by the novel, all-digital measurement system developed at NIST in the past few years.

The addition of a third time scale will provide increased redundancy for the entire time-scale operation, and the fundamentally different technology at the core of the digital measurement system (with respect to the ones presently used to provide the data for AT1 and TSC) will serve as a discriminating tool for the occasional aberrant behavior of the measurement systems. In fact, different technologies usually have different shortcomings that are often triggered by different occurrences.

II. The Measurement of Phase Differences

The high stability of the clocks involved in time-scale operations requires high-resolution measurement systems, making it impossible to use currently available time-interval or frequency counters without the use of sensitivity-enhancing techniques. The traditional and our all-digital sensitivity-enhancing techniques are briefly described below.

A. The dual-mixer technique

The technique traditionally used to compare the phase of two (or more) atomic frequency standards is referred to as dual-mixer measurement technique [1], [2] and is illustrated in its basic conception in Fig. 1.

The mixers in Fig. 1(a) simply down-convert each of the clocks' signals (generally at 5 MHz) to a much lower frequency (generally at 10 Hz) to increase the effective resolution of the time-interval counter. In fact, the phase difference in radians between the two 5 MHz waveforms amounts to the same number of radians for the 10 Hz waveforms, resulting in a time difference which is $5\cdot10^5$ times larger. A time-interval counter with a resolution of 10 ps used in this manner will therefore yield an effective resolution of about $2\pi\cdot10^{-9}$ rad for the phase measurement of the 5 MHz signal.

To first order the quality of the synthesized intermediate frequency (4.999990 MHz in this case) is irrelevant, because its noise contributions are common to both down-converting

processes and therefore cancel out, resulting in easier implementation of this measurement scheme.
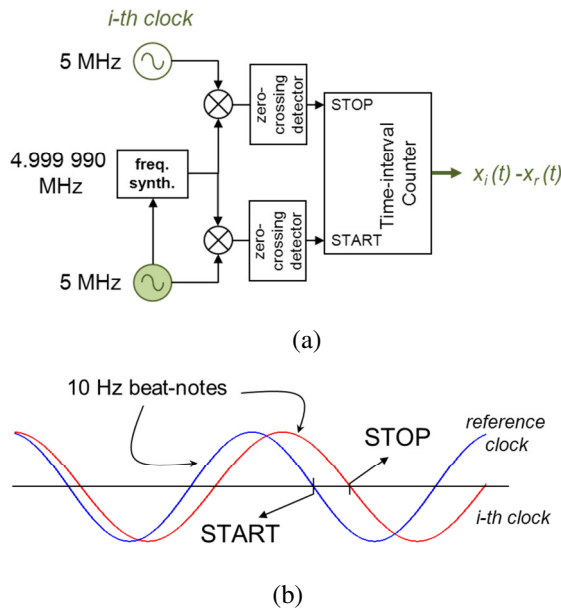

(a)

(b)

Figure 1. The dual-mixer technique for measuring phase differences between two signals. (a) The down-converting mixers produce two beat-note signals used to measure the time (phase) difference. (b) The two down-converted signals and their relation with the start and stop of the time-interval measurement.

The basic concept depicted in Fig. 1 can be expanded to simultaneously measure phase differences between *n* clocks and a common reference.

B. The All-digital technique

The all-digital technique for measuring phase differences between clocks can be summarized in one basic concept: the down-conversion performed by the analog mixers in Fig. 1 is replaced by digital sub-sampling of the clock signals [3]. The result of this operation is a digitized signal that is fitted by a sinusoidal waveform at a much lower frequency than that of the original clock signal.

The sub-sampling operation, like frequency mixing, preserves the signal's phase at the beginning of each measurement instance, allowing the measurement of the phase of a 5 MHz clock signal with a sensitivity gain similar to the one described for the dual-mixer technique.

In Fig. 2 is shown a graphical representation (not to scale) of the sub-sampling process used in the all-digital phase measurement system. The nominal 5 MHz clock signal is sampled at the rate set by the sampling time base square-wave for the duration of the measurement window, providing a set of samples that will be fitted by a sinusoidal waveform that is at a much lower frequency than both the sampling rate and the clock's frequency.

The frequency of the "beat-note" is determined by the residual of the ratio between the clock's frequency (5 MHz) and the sampling rate, which in fact must not be an integer fraction of 5 MHz.
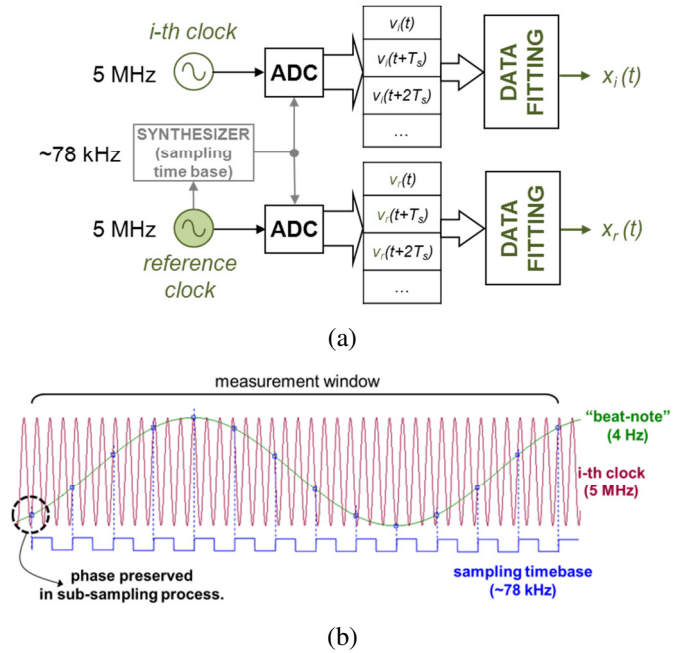

(a)

(b)

Figure 2. (a) Phase measurements using the all-digital technique. A synthesized sampling time base drives the subsampling process and the resulting samples are then fitted by a sinuoisdal waveform. The initial phase of this waveform is the final result of the measurement. (b) Not-to-scale representation of the sub-sampling process. The 5 MHz signal (in red) is sampled at the rate set by the sampling timebase square-wave (which must not be an integer fraction of the nominal 5 MHz) producing a set of samples indicated by the blue squares. These samples are then fitted by a sinusoidal waveform whose frequency is much lower that 5 MHz. The phase of the 5 MHz signal at the beginning of the measurement window is preserved by the sub-sampling process.
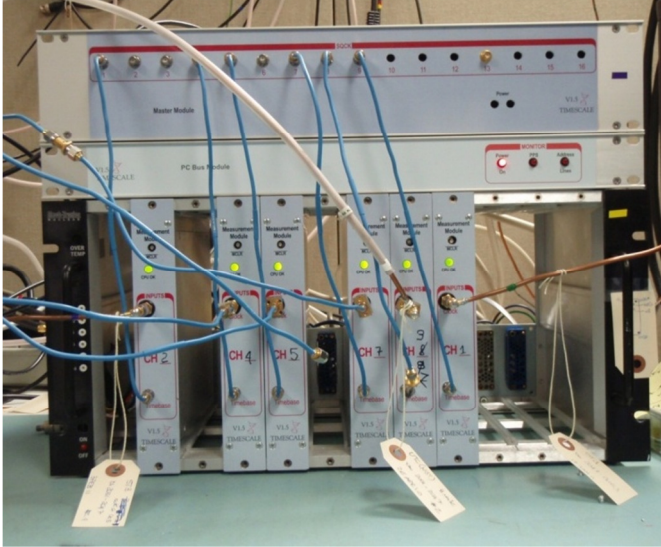
The length of the measurement window is a free parameter that can be chosen together with the sampling rate to determine the number of samples acquired for each measurement instance. The sampling rate and the length of the measurement window are parameters that should be chosen with some care. In fact, if a higher number of samples available for the "beat-note" fitting generally means a higher accuracy in the waveform's initial phase, a longer measurement window may result in a set of samples whose statistical properties are no longer stationary, introducing a bias in the determination of the waveform initial phase.
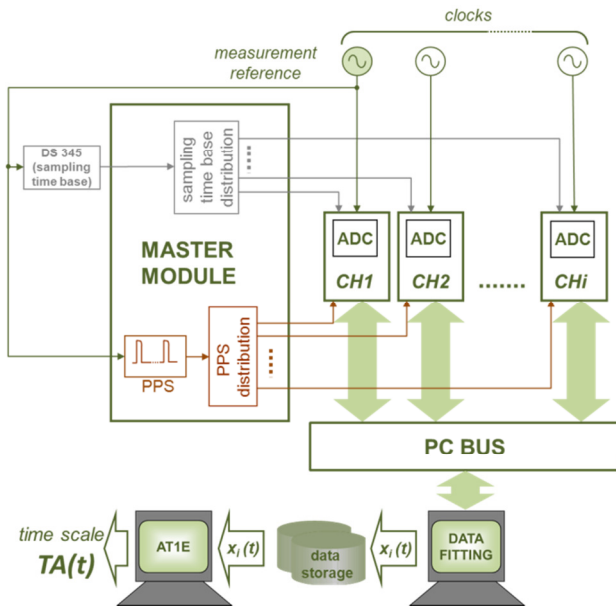
III. THE ALL-DIGITAL MEASUREMENS SYSTEM

The all-digital measurement system presently implemented at NIST is a re-engineered version (V1.5) of the prototype (V1) described in [3] and it can be seen in the photograph shown in Fig. 3(a).

The three main system components are a Master Module (top enclosure), a PC Bus (second enclosure from the top) and the crate housing the six active acquisition modules. The same three components are also indicated in the functional block diagram in Fig. 3(b). One of the clocks under measurement is used to synthesize both the sampling time-base and the pulse-per-second (PPS) signal used to trigger the measurement instances of the system, making that clock the reference for the measurement system. The sampling time-base is not an integer fraction of the nominal 5 MHz frequency of all clocks'

signals, so as an intermediate step towards full Master Module implementation with a Digital Direct Synthesizer (DDS) a commercial synthesizer was used. Both the sampling time-base and the PPS signals are distributed by the Master Module to all acquisition modules indicated as CH1, CH2 and CHi in the diagram.

(a)

(b)

Figure 3. (a) Photograph showing the re-engineered measurement system V1.5. The top enclosure is the Master Module, the second enclosure from the top is the PC Bus, and the crate below them houses the six active acquisition modules. (b) Functional block diagram of the same sytem. The sampling time base and the PPS signal are synthesized from one of the available clocks, which is then the reference clock for the measurement system.

The PC Bus allows the PC dedicated to data fitting to poll in turn each acquisition module, reading the acquired samples from the flash memory chip where they were stored by the microcontroller managing the acquisition process. At the end of the fitting process the phase of each 5 MHz signal at the beginning of each measurement instance, $x_i(t)$, is stored to be processed at a later time by the time-scale algorithm of choice.

Because any time-scale algorithm is substantially a prediction algorithm for clock *differences*, one of the ensemble's clocks is chosen to be the reference clock for the time-scale calculations. This reference clock must not be confused with the clock that is used as the *measurement reference* as indicated in fig. 3(b): while the two may be chosen to be the same physical clock, their functions are separate and different. Although some measurement systems may not allow a complete freedom of choice in this regard, and despite the setup chosen for the measurements shown in this paper, the conceptually optimal choice should use UTC(NIST) as the *measurement* reference clock. The effect of using, instead, one of the clocks as the *measurement* reference has the effect of introducing a skew in the measured data, due to the drift of that clock with respect to the ensemble clock representing the local UTC. As it turns out, the effect of such drift is of no consequence, as discussed in the next section.

IV. SYSTEM CHARACTERIZATION

The names of the frequency sources (clocks) used in the measurements described in this paper are summarized in Table I, where the channel numbers are indicated for both all-digital (DIG) and dual-mixer-based (AT1, TSC) measurement systems.

TABLE I. SUMMARY OF MEASURED CLOCKS

DIG Channel number	AT1 Channel number	TSC Channel number	Clock name and description
1	30	30	ST004 – Hydrogen maser
2	5	5, 25, 26	ST003 – Hydrogen maser
3	7	7	AOG03 – Auxiliary Offset Generator (ST006 steered by UTC(NIST))
4, 5	13	13	ST0022 – Hydrogen maser (reference for sampling time-base, PPS)
7	18	18	ST006 – Hydrogen maser
-	17, 24	17, 24	HP1074 –Cs thermal-beam clock

There are several ways to characterize this measurement system, each one of them providing different and complementary information about its overall performance in the domain of time-scale applications.

A. Common-clock Measurements

In a common-clock measurement, two distinct channels (acquisition modules) measure the same clock, thereby offering as a result the residual noise of each channel, summed in quadrature. Presuming the two measuring channels are virtually identical, the resulting "noise floor" for each of them is assumed to have a total time deviation (or a total fractional frequency deviation) that is 0.7 times better than the one computed from the measured noise levels.

Several results for this configuration are shown and compared for different measurement systems in Fig. 4, where the quantity depicted is the total time deviation (total TDEV)

computed from the measured noise, without the 0.7 factor reduction.

Fig. 4(a) shows the time instability of channels 4 and 5 for the all-digital measurement system (V1.5), as compared with the results of similar measurement for channels 17 and 24 of the dual-mixer-based system that is the core of UTC(NIST). The all-digital system exibits a time instability below 1 ps for measurement periods up to approximately 10 days, and it is comparable with, or better than, the dual-mixer system. The measurements were conducted between MJD 55560 and 55680.

* Glitches removed are > 5 s and amount to less than 3·10-3 of total data points

(a)

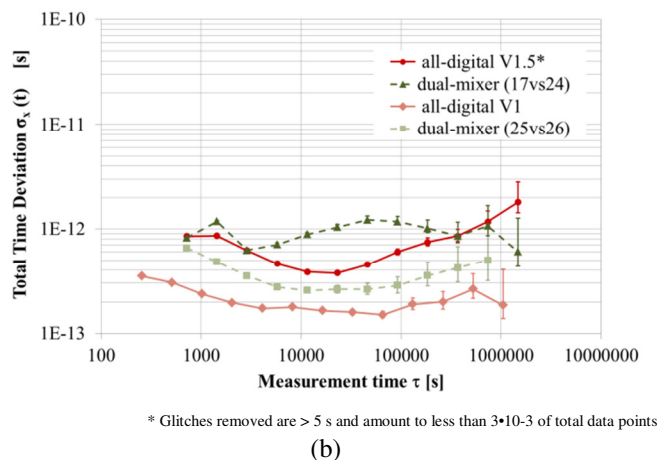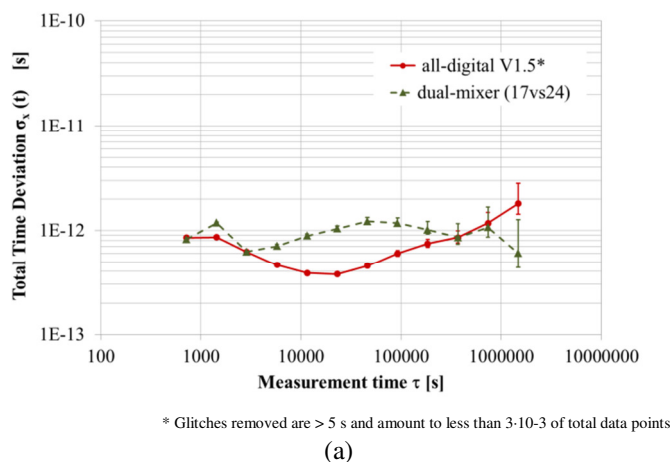* Glitches removed are > 5 s and amount to less than 3•10-3 of total data points

(b)

Figure 4.   (a) Total time deviation calculated for channels 4 and 5 for the all-digital measurement system (V1.5), as compared with the results of similar measurement for channels 17 and 24 of the dual-mixer-based system that is the core of UTC(NIST). (b) Total time deviation calculated for common clock measurements using the prototype all-digital system prior to its re-engineering and a different pair of channels of the dual-mixer system, compared with the data in (a).

In Fig. 4(b) the same data are shown together with the results from common clock measurements using the prototype all-digital system (V1) prior to its re-engineering. Data from a better-performing pair of channels for the dual-mixer measurement system (for the same period spanning approximately MJD 55350-55400) are also shown.

The discrepancy between the two sets of measurements illustrates the dual-mixer system channel-to-channel

performance variability and the unwanted effect of the re-engineering process of the all-digital system, which significantly raised its noise floor, albeit without invalidating its viability for time-scale applications.   In fact, even the worse performance is still within the spread of performance of the dual-mixer system generating UTC(NIST).

Finally, a comparison of the projected effect of using a specific clock as measurement reference clock, instead of UTC(NIST), is compared with the noise floor of the system and determined to be inconsequential, at least for the measurement periods described in this paper. In fact, if the measured drift of ST006 (used as the measurement reference clock) is approximately $-1.27 \cdot 10^{-21}$, after 100 days of measurements the 720 s measurement interval will have an error of approximately 10 fs. This would be the timing error of the measurement system if it were otherwise noiseless: in reality it is well below even the best noise floor of the all-digital measurement system.   The measurement reference clock drift with respect to UTC(NIST) is a negligible contribution to the all-digital system for measurement periods up to 2000 days.

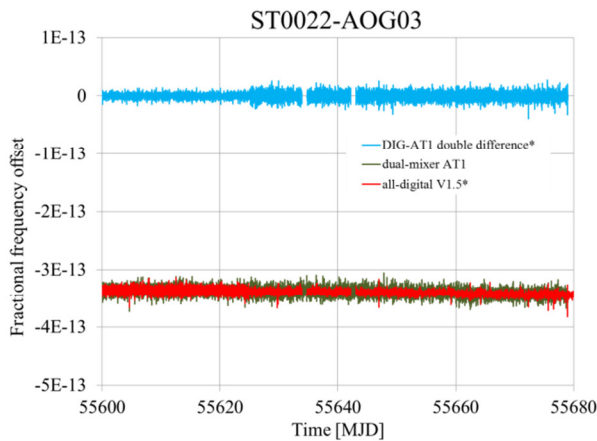### B. Frequency Offset and Double-difference Measurements

Although the common-clock measurements are very important in determining the capabilities of the measurement system, its typical operating conditions require the simultaneous measurement of n different clocks' phases.

Apart from channels 4 and 5, all other active channels in the all-digital measurement system are measuring different clocks (see Table I).   The measurement of the absolute frequency of a clock happens only through its comparison with a primary frequency standard.   The clocks that constitute a time scale are all secondary standards, so any time scale algorithm is essentially a predictor for clock *differences*. In Fig. 5, therefore, is shown one example of the frequency offset (difference) between maser ST0022 and the output of the AOG03, as measured by the all-digital measurement system and the dual-mixer-based one, AT1 in this case.   The blue curve (around zero) is the difference between the same frequency offset, as measured by the two systems: it represents the combined residual noise of the two measurement systems and is obtained by calculating the difference between the red and the green curve of Fig. 5:

double diff. = $(\text{ST0022-AOG03})_{\text{DIG}} - (\text{ST0022-AOG03})_{\text{AT1}}$
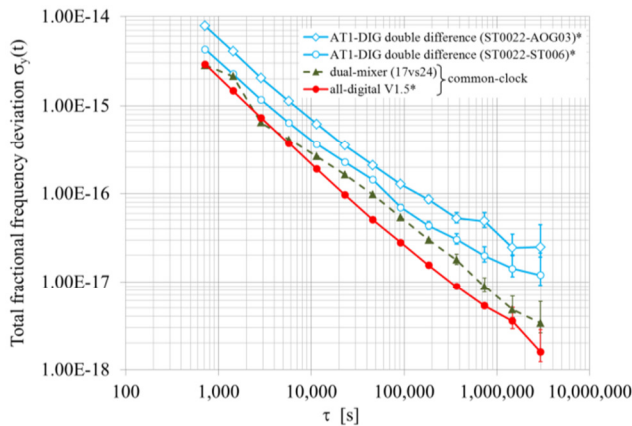
The data in Fig. 5 are representative of the frequency offsets measured between all other clocks listed in Table I: they confirm the ability of the measurement system to accurately measure phase differences evolving with time.

An evaluation of this accuracy is shown by the total fractional frequency deviations shown in Fig. 6, where the combined residual noise of both measurement systems is compared with the common-clock measurements for each one of the measurement systems. The total fractional frequency deviation for the common-clock measurements is computed from the same sets of data used to compute the TDEV shown in Fig. 4.

ST0022-AOG03

Figure 5.   Measurement results for the frequency offset (difference) between maser ST0022 and AOG03, as measured by the all-digital system (red curve) and the dual-mixer-based one (green curve). The blue curve is the difference between the red and the green curves, and it represents the combined residual noise of the two measurement systems.

Figure 6.   Total fractional frequency deviation computed for the common-clock measurements (same data sets used for the TDEV shown in Fig. 4, red and green curves) and for the combined residual noise of the two measuremetn systems, for two different frequency offsets: ST0022-AOG03 and ST0022-ST006. The combined residual noise is obtained by subtracting the frequency offset of each clock pair as measured by each measurement system.

In particular, two double differences are shown in Fig. 6, for two different pairs of clocks: (ST0022-AOG03) and (ST0022-ST006).   The residual noise calculated through double differences is expected to be $\sqrt{2}$ above the noise of a common-clock measurement, because the noise of each pair of channels is summed in quadrature. The differences between the two double difference curves in Fig. 6 (empty circles and empty diamonds) is due to the variability between the each channel's noise floor, as shown by the difference between the results of common-clock measurements between different pairs of channels of the same dual-mixer-based measurement system.

The interesting feature of Fig. 6 is in the flicker-type behavior shown by both the double difference curves, but not by the curves based on common-clock measurements. At this time it is not clear what the cause of it is, and it is currently under investigation.

V.   CONCLUSIONS AND FUTURE WORK

The performance of the re-engineered, multi-channel, all-digital measurement system presently active at NIST is presented, and compared, for both common-clock performance and operational (difference clocks) performance with the dual-mixer-based system that is at the core of UTC(NIST).

Apart from validating the all-digital system as fit to be used as part of an operational time scale, the comparison between the measurements obtained from both systems offers the possibility to investigate long-term behaviors not seen previously, as shown in Fig. 6.

Future work includes reducing the residual noise for the all-digital system in order to reach the levels warranted by the prototype V1, implementing ancillary systems allowing for automated processing of the data into a time-scale algorithm, and investigating the long-term trends of both measurement systems.

REFERENCES

[1]   D. Allan, H. Daams, "Picosecond time difference measurement system," Proceedings of the 1975 International Frequency Control Symposium, pp. 404-411.

[2]   S. Stein, et al., "Automated high accuracy phase measurement system," IEEE Transactions on Instrumentation and Measurement, Vol. 32, pp. 227-231, 1983.

[3]   S. Römisch, T.E. Parker, S.R. Jefferts, "Novel, all-digital phase measurement system for time scales," Proc. of the 41st PTTI Meeting, pp. 397-408, 2009.